

Coherent phonon oscillations in GaAs

A. V. Kuznetsov and C. J. Stanton

Department of Physics, University of Florida, Gainesville, Florida 32611

(Received 29 June 1994; revised manuscript received 16 November 1994)

We present a microscopic theory of plasmon-phonon oscillations created by ultrafast optical excitation in polar semiconductors. Our analysis is based on the equations for the optical lattice displacement and the electronic polarization. For an idealized situation with homogeneous plasma density we find that plasmonlike oscillations dominate the transient behavior after the optical excitation. However, once the inhomogeneous density distribution is taken into account, only density-independent LO-phonon oscillations are present in the transient optical response. By using a model of electro-optical response that includes the influence of both the electric field and the lattice displacement on the refractive index, we achieve a quantitative agreement with the experiment.

I. INTRODUCTION

Recent experiments¹⁻⁶ have shown that ultrafast optical excitation can coherently excite optical phonon modes in semiconductors. Oscillating changes in optical properties have been observed in GaAs,^{1,2} Ge,³ and a number of other materials.^{4,5} A thorough discussion of the experimental techniques and a complete bibliography can be found in a recent review.⁶

In materials with low crystal symmetry phonon oscillations are caused by deformational electron-phonon coupling which makes a finite value of the lattice displacement energetically favorable after the excitation. The sudden increase in the photocarrier density during the femtosecond excitation makes the lattice oscillate around the new equilibrium position.^{4,7,8} However, this "displacive" mechanism can only work in materials where isotropic electron density distribution can deform the lattice along some preferential crystallographic direction, and only A_1 phonon modes that do not reduce the lattice symmetry can be excited in this way.^{4,7}

Coherent optical phonon oscillations are quite pronounced in GaAs,^{1,2} where experiments suggest another mechanism for coherent phonon excitation. It has been shown experimentally that the amplitude of the oscillations in polar materials is related to the strength of the electric field in the depletion region near the surface of the sample. In a polar material, the electric field interacts with both optical phonons and electrons. After the optical excitation the photocarriers will separate in the electric field, creating electronic polarization. This polarization will, in turn, affect the field and may cause the lattice to oscillate.

Although the transient screening of the depletion field by photocarriers has been unambiguously identified as the driving force for phonon oscillations,^{1,2,9-13} it should also drive *plasmon* oscillations even in a nonpolar material. In polar materials, where plasmons and LO phonons combine into plasmon-phonon modes with density-dependent frequencies,¹⁴ one can expect both modes to be excited by ultrafast screening. While experiments clearly show oscillations with the LO-phonon frequency, it is

surprising that there is no trace of plasmon oscillations, nor is there any density dependence of the observed oscillation frequency at densities up to 10^{18} cm^{-3} .

The existing theoretical approaches neglect the plasmon degree of freedom in their treatment of electron dynamics. Scholz and Stahl¹³ have considered the evolution of the depletion field after ultrafast photoexcitation taking into account lattice polarization macroscopically. Kurz and co-workers have performed numerical simulations based on the drift-diffusion model⁹⁻¹² which describes the slow component of the observed optical response very well. However, neither of the models adequately describes the experimentally observed oscillations.

In the present paper we develop a microscopic theory of plasmon-phonon oscillations. The plasmon-phonon equations for a uniform case are solved in Sec. II, where we also discuss differences in the oscillatory behavior of the electric field and the lattice displacement. In Sec. III we consider the case of a nonuniform density distribution which is more appropriate for the description of experiments^{1,2} performed with tightly focused laser beams, and compare the results with experiment. We also discuss the possibility of terahertz emission by coherent phonons. The final section, Sec. IV, contains concluding remarks.

II. DYNAMICS OF PLASMON-PHONON MODES FOR UNIFORM PHOTOEXCITATION

In this section we will study the plasmon-phonon dynamics for the case of spatially uniform density of photoexcitations. This generic case of homogeneous density and uniform applied field is important for understanding the physics of the transient response, although it may not be directly applicable to realistic experiments.

Our analysis is based on the well-known equations for plasmon-phonon modes which in the time domain read¹⁴

$$\frac{\partial^2}{\partial t^2} \mathbf{P} + \gamma_{\text{el}} \frac{\partial}{\partial t} \mathbf{P} + \omega_{\text{pl}}^2 \mathbf{P} = \frac{e^2 N(r)}{\epsilon_{\infty} \mu} [\mathbf{E}^{\text{ext}} - 4\pi \gamma_{12} \mathbf{W}], \quad (1)$$

$$\frac{\partial^2}{\partial t^2} \mathbf{W} + \gamma_{\text{ph}} \frac{\partial}{\partial t} \mathbf{W} + \omega_{\text{L}}^2 \mathbf{W} = \frac{\gamma_{12}}{\epsilon_{\infty}} [\mathbf{E}^{\text{ext}} - 4\pi \mathbf{P}]. \quad (2)$$

Here, \mathbf{P} is the electronic polarization and W is the normalized lattice displacement ($W = \sqrt{\rho}u$, where u is the displacement of the optical mode and ρ is the reduced density). In the absence of coupling, the polarization is expected to oscillate with the plasmon frequency $\omega_{\text{pl}} = \sqrt{4\pi e^2 N / \epsilon_\infty \mu}$ (N being the total density of carriers and μ the reduced electron-hole mass), while the frequency of lattice oscillations should be that of the longitudinal optical phonon ω_L . The coupling of phonons to the electric field is characterized by $\gamma_{12} = \omega_T \sqrt{(\epsilon_0 - \epsilon_\infty) / 4\pi}$, where ϵ_0 and ϵ_∞ are the low- and high-frequency dielectric constants, and ω_T is the transverse phonon frequency.¹⁵

Note that, because both optical phonons and plasmons are dispersionless, the equations are the same for all wave vectors except $\mathbf{q} = \mathbf{0}$, where the uniform applied field E^{ext} creates a driving force on the right-hand side of both equations. If the field is nonuniform as is the case in the surface depletion layers, the driving term will be finite also in a small vicinity of $\mathbf{q} = \mathbf{0}$. However, the corresponding range of wave vectors is of the order of the inverse depth of the depletion layer (about 100 nm), so that it is very small compared to the size of the Brillouin zone. Therefore we can restrict ourselves to considering only the zero-wave-vector mode.

The decay of the oscillations is described by phenomenological relaxation terms in (1) and (2). The relaxation constant for electronic polarization has the meaning of the momentum relaxation time, which can be as short as a few tens of femtoseconds. The constant that describes damping of phonon oscillations is related to the anharmonic decay time for LO phonons (about 4 ps).¹⁶

These equations describe two coupled harmonic oscillators. The frequencies of the normal modes of this system are shown in Fig. 1 for GaAs parameters ($\epsilon_0 = 12.9$, $\epsilon_\infty = 10.9$, $\nu_{\text{LO}} = 8.76$ THz, $\nu_{\text{TO}} = 8.06$ THz, and $\mu = 0.06m_{\text{el}}$) as a function of plasma density. At very low densities the plasmon branch is overdamped, and the phonon branch has the LO frequency. At very high densities, the fast plasmon oscillations screen the longitudinal field associated with the lattice motion, reducing the

phonon frequency to that of the TO phonon. The anticrossing of both branches occurs at densities around 10^{18} cm^{-3} , where both modes become strongly damped. Except for a small effect of damping on the frequencies, Fig. 1 is identical to the well-known results of Ref. 14.

In the presence of the external electric field, these equations also have steady-state solutions:

$$P = 0, \quad W = \frac{\gamma_{12}}{\omega_L^2 \epsilon_\infty} E^{\text{ext}} \quad (3)$$

for zero density before the excitation, and

$$P = \frac{E^{\text{ext}}}{4\pi}, \quad W = 0 \quad (4)$$

after the excitation pulse has created a nonzero carrier density in the sample. The system will react to the optical excitation by moving from one equilibrium position (3) to the other (4). Because both the lattice and the electrons possess a certain inertia represented by second-derivative terms in (1) and (2), the system will oscillate around the new equilibrium position. Both plasmon-phonon modes shown in Fig. 1 should be involved in the oscillatory transient.

Unfortunately, in general it is not possible to describe this transient behavior analytically because of the way the time-dependent carrier density enters Eq. (1): it affects the source term in the right-hand side and the plasmon frequency, so that solutions of (1) are nonlinear in the density even in the absence of phonons [note that the plasmon-phonon coupling is also proportional to the density through the prefactor on the right-hand side of (1)]. However, an approximate analytical solution can be obtained in the limit of very low densities, where we can leave out the coupling between the two equations, and neglect the time dependence of the plasmon frequency.

We will describe the evolution of the density by a simple rate equation,

$$\frac{dN}{dt} = N_0 I(t), \quad (5)$$

where N_0 is the final value of the density, and $I(t)$ is the temporal profile of the excitation intensity normalized in such a way that

$$\int_{-\infty}^{+\infty} dt I(t) \equiv I(\omega = 0) = 1. \quad (6)$$

This equation represents the process of optical generation of carriers. We do not include recombination in (5) since it occurs in a much longer time scale (tens of nanoseconds).

In the low-density limit the equations are uncoupled, so that we can solve the plasmon equation (1) first and then substitute the resulting solution for the polarization into (2). If we further assume that the excitation duration is much shorter than the characteristic rise time of the polarization (the plasmon period), we can neglect the time dependence of the plasmon frequency on the left-hand side of (1). Under these simplifications, we can immediately write down the Fourier-transformed solution:

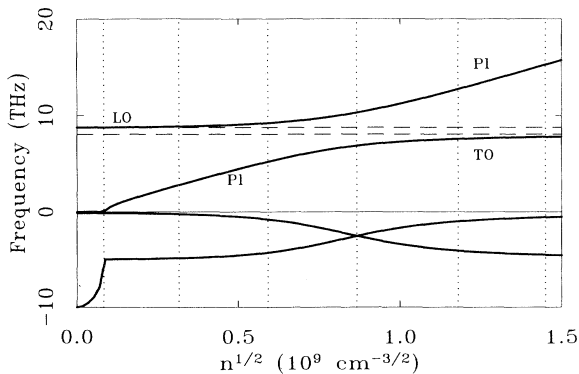


FIG. 1. Density dependence of plasmon-phonon mode frequencies in GaAs. The two bottom curves with negative frequencies show the density-dependent dephasing of both modes calculated for $\gamma_{\text{el}}^{-1} = 0.1$ ps and $\gamma_{\text{ph}}^{-1} = 4$ ps. Vertical dotted lines mark density values used in numerical solutions below.

$$iP(\omega) = \frac{\omega_{\text{pl}}^2 E^{\text{ext}}}{4\pi} \frac{I(\omega)}{(\omega + i\delta)(\omega_{\text{pl}}^2 - \omega^2 + i\gamma_{\text{el}}\omega)}. \quad (7)$$

The denominator of (7) is a third-degree polynomial, so that the solution has three poles in the frequency domain. Consequently, in the time domain the solution will be the sum of three oscillating terms with the frequencies 0 and $\pm\omega_{\text{pl}}$ (for simplicity, let us assume that the dephasing is zero; finite dephasing will only add a small imaginary part to the plasmon poles):

$$P(t) = \frac{\omega_{\text{pl}}^2 E^{\text{ext}}}{4\pi} \{1 - I(\omega_{\text{pl}}) \cos[\omega_{\text{pl}} t]\} \theta(t) \quad (8)$$

(it is valid only after the pulse is over). Substituting (7) as a source term into (2), we get for the Fourier transform of the displacement,

$$W(\omega) = -\frac{\gamma_{12} \omega_{\text{pl}}^2 E^{\text{ext}}}{\epsilon_{\infty}} \frac{I(\omega)}{(\omega + i\delta)(\omega_{\text{pl}}^2 - \omega^2)(\omega_L^2 - \omega^2)} \quad (9)$$

[the constant component (3) has been left out]. Again, the denominator is a polynomial, so that in the time domain the solution is a superposition of three oscillating components:

$$W(t) = \theta(t) [W_0 + W_{\text{pl}} \cos \omega_{\text{pl}} t + W_{\text{ph}} \cos \omega_L t], \quad (10)$$

with

$$W_0 = -\frac{\gamma_{12} E^{\text{ext}}}{\epsilon_{\infty} \omega_L^2}, \quad W_{\text{pl}} = W_0 I(\omega_{\text{pl}}) \frac{\omega_L^2}{\omega_L^2 - \omega_{\text{pl}}^2}, \quad (11)$$

$$W_{\text{ph}} = -W_0 I(\omega_L) \frac{\omega_{\text{pl}}^2}{\omega_L^2 - \omega_{\text{pl}}^2}.$$

We see that the constant component exactly offsets the initial displacement (3); the component at the plasmon frequency is of the order of the initial displacement and may even exceed that, while the component at the LO frequency is small (quadratic in plasma frequency, i.e., linear in N , and further scaled down by the excitation spectral density at the phonon frequency). In the same approximation, we can write down for the electric field

$$E(t) = E^{\text{ext}} - 4\pi P - \gamma_{12} W$$

$$= E^{\text{ext}} - \theta(t) [E^{\text{ext}} + E_{\text{pl}} \cos \omega_{\text{pl}} t + E_{\text{ph}} \cos \omega_L t] \quad (12)$$

with

$$E_{\text{pl}} \approx E^{\text{ext}} I(\omega_{\text{pl}}), \quad (13)$$

$$E_{\text{ph}} = E^{\text{ext}} I(\omega_L) \frac{\omega_{\text{pl}}^2}{\omega_{\text{pl}}^2 - \omega_L^2} \left[\frac{\epsilon_0 - \epsilon_{\infty}}{\epsilon_0} \right].$$

We see that both the lattice displacement and the electric field are superpositions of a constant background with oscillations at plasmon and phonon frequencies. However, the relative magnitudes of oscillations in these two quantities are very different. Comparing (11) with (13), we have

$$\frac{W_{\text{ph}}}{E_{\text{ph}}} = \frac{W_0}{E^{\text{ext}}} \left[\frac{\epsilon_0}{\epsilon_0 - \epsilon_{\infty}} \right]. \quad (14)$$

According to (14), an oscillatory electric field at the phonon frequency produces a displacement which is about an order of magnitude larger than the constant displacement (3) caused by a constant field of the same magnitude. Due to this resonant enhancement, the lattice displacement (10) is no longer proportional to the electric field (12) as is the case for constant (or slowly varying) field.

The above analytical results are of limited practical value because the approximations we made are too crude (e.g., the results would diverge at the next step of the iterative procedure because we have neglected mode coupling). However, the qualitative trends that we have discussed in connection with this approximate solution are borne out by numerical results that are presented below.

The system of equations (1) and (2) poses little computational challenge. We have solved it numerically for the parameters of GaAs (see Fig. 1), assuming a Gaussian excitation pulse with 50 fs full width at half maximum (FWHM), and the magnitude of the external dc field set to 100 kV/cm (the results are linear in the dc field, so this choice does not really matter). The solutions and their Fourier transforms are shown in Figs. 2–5.

Figure 2 shows the evolution of lattice displacement W at different excitation densities; Fig. 3 displays the Fourier transforms of these curves. At low densities, the

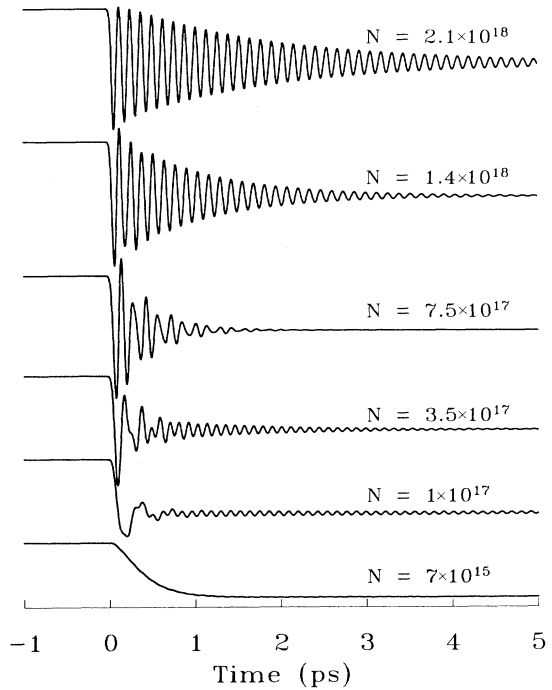


FIG. 2. Transient behavior of the lattice displacement after ultrafast optical excitation at different excitation densities indicated by dotted lines in Fig. 1. After the initial displacement has been compensated, the lattice oscillates around $W=0$. Note the mode beating at intermediate densities due to the presence of two plasmon-phonon modes.

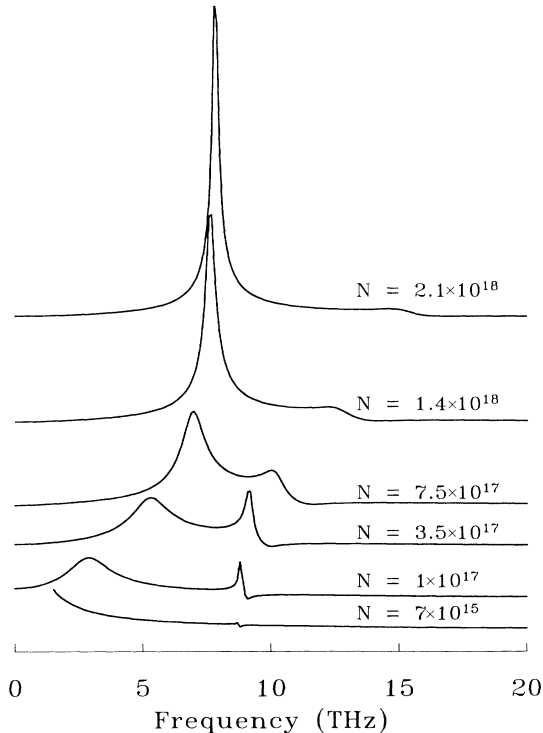


FIG. 3. Fourier transforms of the lattice displacement curves shown in Fig. 2. The transition from weak LO oscillations to strong TO oscillations at high densities is evident. In the anticrossing region ($N = 7.5 \times 10^{17} \text{ cm}^{-3}$) both modes show strong damping that results in the suppression of the oscillations in the time domain.

amplitude of the phonon oscillations is small while the plasmon oscillations are of the order of the initial displacement. At intermediate densities, the phonon oscillations shift to higher frequencies and both modes become strongly damped (cf. Fig. 1). At high densities, the high-frequency branch (plasmons) no longer shows in the lattice displacement because the plasmons become too fast for the lattice to be able to respond to their motion. Instead, the fast plasmons are now able to adiabatically follow lattice oscillations, which results in the disappearance of LO oscillations and the emergence of a strong TO peak. The magnitude of the TO oscillations at high densities is practically equal to the initial displacement, which is the theoretical limit for a shifted oscillator that is released instantaneously.

The results for the electric field shown in Figs. 4 and 5 confirm the analytical argument that the dynamical behavior of the field can be very different from that of the displacement. The LO-phonon oscillations are much less pronounced in the field dynamics, in agreement with the estimate (14). Also, at higher densities the field has a high-frequency plasmon component that does not appear in the lattice dynamics.

In summary, the results of this section indicate that in a spatially homogeneous situation it is quite difficult to excite LO-phonon oscillations. For the above-discussed reasons, LO oscillations are more pronounced in the lat-

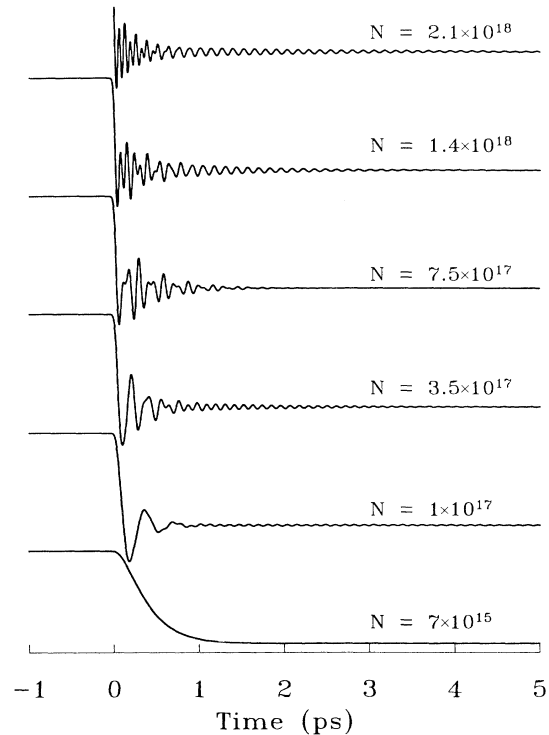


FIG. 4. Time dependence of the electric field (14) for the conditions of Fig. 2. Again, after the applied field is screened, there are oscillations around zero field. However, the relative magnitude of the two modes is different from that in the case of displacement.

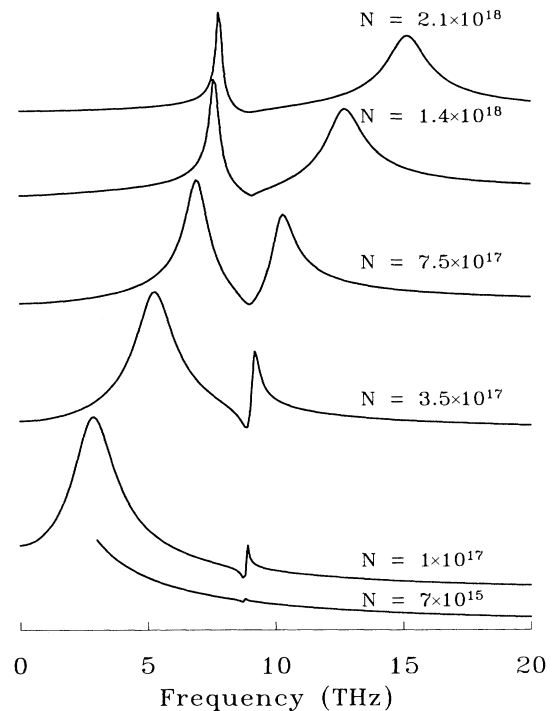


FIG. 5. Fourier transforms of the field from Fig. 4. Note that the high-frequency plasmons are quite pronounced in the field at high densities, and that at low densities the LO peak is very weak.

tice displacement than they are in the field dynamics, but still they are weak compared to the plasmons, in agreement with the analytical estimates (11) and (13). There are two physical reasons for that: (a) LO phonons are only present at low densities, where the rise time of the polarization (the plasmon period) is long, so that the lattice has time to adjust adiabatically to the time-dependent field; (b) the factor $I(\omega_L)$ in (11) and (13) further reduces the LO amplitude by a factor of 3 for a 50 fs pulse.

This result apparently disagrees with experiment. In the next section we will show how the experiments can be quantitatively explained in spite of this apparent contradiction.

III. COMPARISON TO EXPERIMENT

We will concentrate on the experiments conducted by Kurz and co-workers.^{1,2,9,10} A typical set of experimental data is shown in Fig. 6, where the observed reflective changes are plotted versus probe delay time for different excitation densities. The change in the reflection coefficient is thought to represent the time-dependent electric field directly via the electro-optic effect.^{1,2,9,10}

To begin with, let us point out three features of the experimental data that are most important for our analysis. (1) The frequency of oscillations is independent of the density and is equal to that of the LO phonon; (2) there is no trace of plasmon oscillations in any of the curves, even though they cover two orders of magnitude in the density; (3) the amplitude of the oscillations never exceeds 10% of the overall reflective change. All three features are in direct contradiction to the analysis of the preceding section, where we have shown that the oscillation frequency should be density dependent, the plasmons should be more pronounced than the phonons, and the amplitude of lattice oscillations can be of the order of the initial displacement.

In this section we are going to demonstrate that these contradictions can be eliminated by taking into account the differences between the realistic experimental situation and the idealized case considered above.

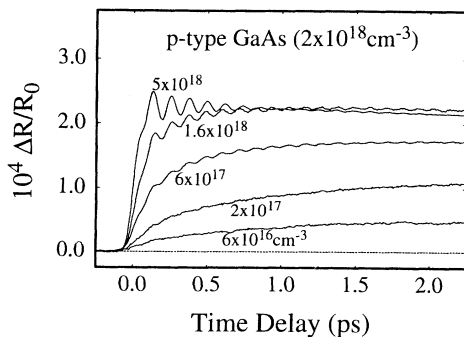


FIG. 6. Experimentally observed reflective changes in *p*-doped GaAs at different excitation densities. Reprinted with permission from Ref. 10.

Inhomogeneous density distribution

In the experiment, high excitation densities are produced by tightly focusing the laser beam on the sample.^{1,2} Focusing does produce higher average densities, but also makes it practically impossible to maintain constant density across the illuminated spot. As was pointed out by Collins and Yu,¹⁷ this density inhomogeneity is absolutely crucial to understanding the optical response. In their Raman scattering experiments, they have seen LO and TO scattering peaks instead of density-dependent plasmon-phonon features. To explain their results, they had to integrate the mode spectrum over a wide density range. Because only density-independent features such as LO phonons at low densities and TO phonons at high densities can survive such averaging, the plasmon branch is not observed due to this inhomogeneous broadening effect. Let us stress that this does not mean that the plasmons are not excited, it only means that they cannot be detected because of the interference of plasmons with different frequencies that contribute to optical response from different points in the excited spot.

The situation of Ref. 17 is very reminiscent of the coherent phonon results discussed here, where neither plasmons nor the density dependence of oscillation frequency is observed. The averaging over different densities across the excited spot can be expected to suppress density-dependent plasmon oscillations. The exact way the density averaging should be performed depends on the particular form of the density distribution across the illuminated spot. If the reflectivity R is dependent on the local value of the density $n(r)$, the observed reflectivity can be represented as¹⁷

$$R^{\text{tot}} \propto \int_0^\infty 2\pi r dr R(n[r]) E^{\text{Pr}}(r), \quad (15)$$

where we have also taken into account the spatial distribution of the probe electric field (since the reflected signal is collected by a lens from its focal point, one has to sum the fields and not the intensities from different points). In the case when both the pump and the probe have Gaussian spatial profiles, we can transform (15) into an integral over the density:

$$R^{\text{tot}} \propto \int_0^{N_0} dn \frac{R(n)}{\sqrt{n}} f(n). \quad (16)$$

Here, N_0 is the maximum density at the center of the spot, and the phenomenological form factor $f(n)$ accounts for deviations from the Gaussian profile (it is equal to 1 if the distribution is exactly Gaussian). In the numerical simulations below, we will assume that the form factor changes linearly from 1 at $n=0$ (in the wings of the distribution) to a finite value $C < 1$ in the center of the spot ($C=0.2$ unless stated otherwise). Even without the form factor, it is clear from (16) that the low-density wings, because of their greater area, give a much larger contribution to the overall signal than the small high-density region in the center.

Hot-carrier effects

Another deviation from the simple physical picture of the preceding section is due to band structure effects in

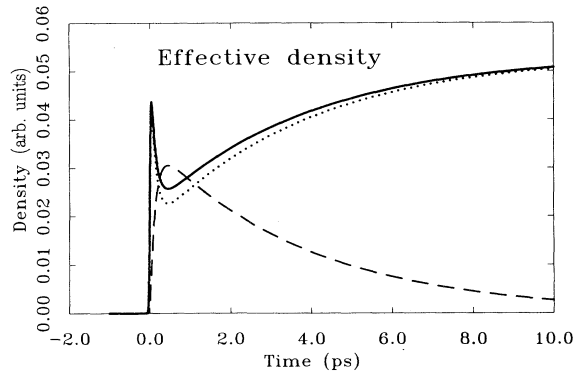


FIG. 7. Time evolution of the electron density in the L -valley (dashed line) and the Γ valley (dotted line). The solid line is the effective density $N^{\text{eff}} = N_{\Gamma} + 0.1N_L$. Calculated according to a rate-equation model of Ref. 18.

GaAs. Optical excitation at 2 eV creates electrons with enough kinetic energy for intervalley transfer, so a substantial part of the total density will be transferred to the L valley immediately after the excitation. Since the ratio of L - to Γ -valley mass is about 10, the L -valley electrons have much lower mobility and are much less effective in screening of the applied field. This effect was shown to be important for the description of the slow component of the optical response.¹⁰

Following the approach of Ref. 18, we assume that the total mobility is proportional to $N^{\text{eff}} = N_{\Gamma} + 0.1N_L$ due to the above-mentioned mass difference between the valleys. We have calculated the time dependence of the densities in different valleys using the rate-equation model of Ref. 18 and used the time dependence of the effective density rather than that of the total density in the subsequent calculations of the optical response. The effective density (Fig. 7) drops immediately after the excitation due to the transfer of carriers to the L valley, and then approaches the total density as the carriers transfer back to the Γ valley with the time constant of about 3 ps.¹⁰

This effect brings the slow component of the calculated response closer to the experimentally observed one and also enhances the amplitude of the oscillations. We did not include more complicated high-field transport effects such as drift velocity saturation,¹⁰ which could have further improved the slow response but are unlikely to affect the oscillations which are our main concern.

Field nonuniformity

In the preceding section we have assumed the applied dc electric field to be spatially uniform. However, in realistic depletion layers the field penetrates only a short distance (some tens of nanometers) below the surface.

We have found that the nonuniform density distribution plays a decisive role in our model because the response is nonlinear in the density. In contrast, the nonuniform field distribution in itself does not affect anything for the simple reason that the response is *linear* in

the field. However, the finite depth of the depletion layer has an indirect effect on the optical response for two reasons. (1) The depletion layer depth w is much smaller than the absorption length l_a (about 300 nm in GaAs at 2 eV). Since the oscillations will be affected by the screening transients only within the depletion layer, while the probe reflection is determined by a much larger region of the thickness l_a , the transient response should be scaled down roughly by a factor w/l_a . A full electrodynamic calculation (e.g., the transfer matrix approach of Ref. 10) is needed to describe this effect quantitatively. (2) In an infinite system, an arbitrarily small density of carriers can screen any applied field by achieving large enough separation distance. However, for a system where the field is present only within a narrow layer of the depth w , the maximum field strength that can be screened by a given density of carriers N is $E_{\text{max}} = 4\pi eNw$. At low densities ($< 10^{16} \text{ cm}^{-3}$) this value can be smaller than the depletion field, so that not all of the available field will be screened. This effect is evident in Fig. 6 where experimental curves at lower densities clearly approach smaller limiting values at long times, which seems to indicate smaller overall field change, i.e., that the screening is incomplete.

Both effects make it difficult to predict the absolute value of the reflective changes due to the lack of reliable information about the depth and field profiles of realistic depletion layers. However, the first effect only scales the response by a constant factor, while the second leads mostly to a density-dependent scaling at low densities. Including realistic field profiles is needed for the description of the slow component of the response, which is determined by the balance of drift and diffusion flow at longer times.¹⁰ In contrast, for the oscillatory response which is determined by a short-time dynamics, we can expect field inhomogeneity to be only marginally important.

In this paper we will treat these geometrical constraints simply by scaling the calculated optical response so that it matches the observed limiting value of the reflective change at long times. The scaling factor turns out to be density independent at higher densities, and has to be reduced at very low densities to account for the incomplete screening in agreement with the above argument.

Electro-optical response

We also have to consider how the experimentally measured quantity (the difference in reflection coefficients for two orthogonally polarized probe components) is related to microscopic quantities in our model. In steady state (or for slowly varying fields) the difference in refractive indices is determined by the electro-optic effect:

$$\Delta n = \frac{1}{2} n_0^3 r_{14} E(t), \quad (17)$$

where r_{14} is the electro-optic coefficient ($1.6 \times 10^{-10} \text{ cm/V}$ for GaAs).¹⁰

However, the lattice displacement also affects the optical properties. We can quite generally write the following phenomenological expression for the reflective change:¹⁹

$$\Delta R/R \propto r^e E + r^w \left[W \frac{\omega_L^2 \epsilon_\infty}{\gamma_{12}} \right]. \quad (18)$$

In the traditional language of electro-optical phenomena, the first term in (18) originates from (fast) electronic “bond charge” response, while the second is related to a slower lattice distortion process (“bond stretching”).¹⁹

In steady state, this expression reduces to (17) with $r_{14} = r^e + r^w$, because in steady state the displacement is proportional to the field [Eq. (3)]. Consequently, for slowly varying fields there is no need to distinguish between the field and the displacement, and the expression (17) can be used to calculate the optical response.

However, as we have seen in Sec. II, the dynamical behavior of the field and the displacement can be very different, so that the more general Eq. (18) is needed to describe the transient optical response. Because field oscillations cause disproportionately large lattice displacement [cf. (14)], the oscillatory optical response will be primarily determined by the second term in (18).

Below we will present results calculated with $r^e = 0$ (the response is determined by the displacement only), $r^w = 0$ (by the field only), and $r^e/r^w = -2.7$, which is a proper choice for GaAs according to Ref. 19.

Numerical results

In our numerical simulation, we solve the plasmon-phonon equations (1) and (2) for 100 density values from N_0 (the value shown on the curves) down to zero. The time dependence of the effective density is determined by the rate-equation model of Ref. 18 (Fig. 7) and is the same for all densities. Then we integrate the calculated field and the displacement according to (16) to account for the inhomogeneous density distribution. The resulting integrated field and displacement are then used to evaluate the optical response according to (18). The curves are scaled to match the observed values of the reflective change at long times. Finally, the results are convolved in time with a 50 fs FWHM Gaussian probe pulse to simulate the detection procedure.

The results of the simulation are shown in Figs. 8–10 for three different choices of the electro-optic coefficients. Figure 8 displays the results for $r^e/r^w = -2.7$, which is the value taken from Ref. 19. The agreement between this set of data and the experimental curves shown in Fig. 6 is remarkably good, especially for the oscillatory part of the response. As we have mentioned earlier, the slow response is influenced by the finite depth of the depletion layer and is much better described by the drift-diffusion model of Ref. 10. However, we are able to reproduce the frequency, amplitude, and phase of the observed oscillations reasonably well.

In the preceding section we have pointed out that it is quite difficult to excite LO-phonon oscillations in a spatially homogeneous situation. However, weak LO oscillations from the low-density wings of the distribution have a constant frequency and add up constructively during the density averaging. In contrast, the plasmon oscillations, which have different frequencies at different densities, tend to cancel out in the density integral, even

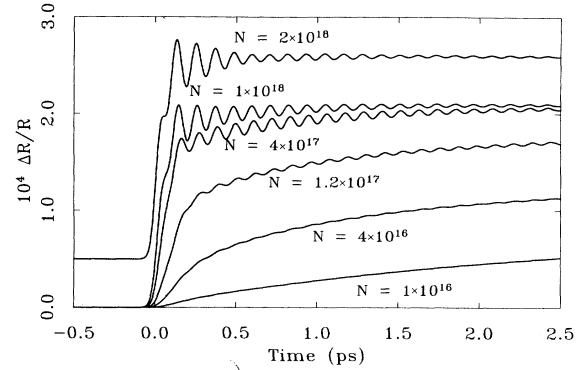


FIG. 8. Time dependence of the differential reflectance for different excitation densities calculated using the procedure described in the text. One of the curves is lifted by 0.5 to avoid overlapping. The ratio of electro-optic coefficients in (18) is $r^e/r^w = -2.7$, which is the value given in Ref. 19 for GaAs.

though at any given density they are stronger than the phonon ones.

Let us also mention that the densities we have used in the simulation are systematically lower than the ones indicated in Fig. 6 by approximately a factor of 5. This may partly be due to our simplified treatment of the hot-carrier transport. For 2 eV excitation and strong dc fields, the effective mass of the carriers may be higher, which would have the same effect as scaling up the densities. Also, the experimental values of the densities may be overestimated due to the uncertainties in the absorption length and the lateral dimensions of the excited spot.

In Fig. 9 we show the reflective response calculated for $r^e = 0$, i.e., under the assumption that the response is determined solely by lattice displacement. Figures 8 and 9 are almost identical, which confirms our claim that the displacement is primarily responsible for the oscillatory response. However, one can see that the oscillations in Figs. 8 and 9 have opposite phases. This is due to the fact that in Fig. 8 the contributions of the electric field and the displacement have opposite sign. For the slow

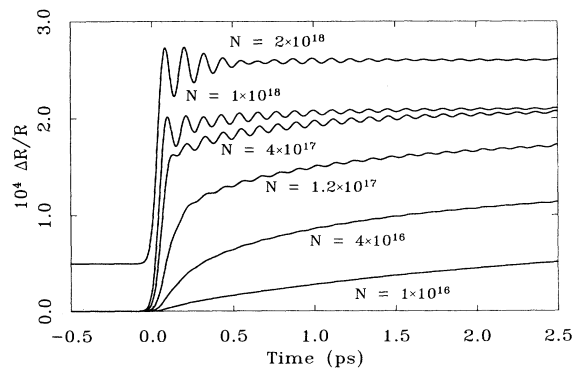


FIG. 9. Differential reflectance calculated with $r^e = 0$, i.e., assuming that the response is affected by lattice displacement only. One of the curves is lifted by 0.5 to avoid overlapping. The response is very similar to that of Fig. 8, but the sign of the oscillatory component is reversed.

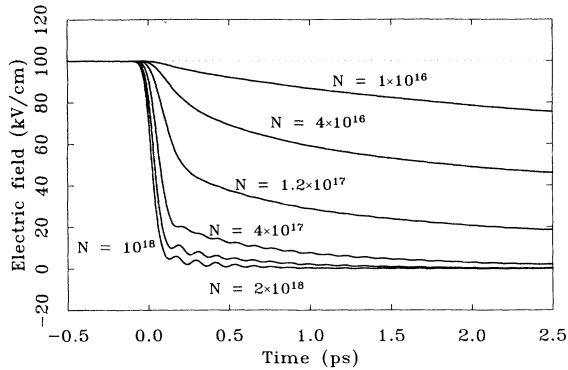


FIG. 10. Temporal evolution of the density-averaged electric field for the conditions of Figs. 8 and 9. The field is also convolved with a 50 fs probe. The oscillations in the field are much smaller than experimentally observed (Fig. 6).

response, the sign of the reflective change is determined by the field contribution, which is larger by a factor of 2.7. However, in the oscillatory part the displacement contribution is increased by a much larger factor due to resonant enhancement, and the overall sign of the response is reversed. In other words, the signs of the effective electro-optic coefficients for the slow response and for the oscillations are opposite. As a result, the oscillations are flipped over in Fig. 9 where both the slow and the oscillatory component have the same sign of the response.

Finally, in Fig. 10 we plot the time dependence of the electric field which would be directly proportional to the differential reflectivity^{1,2,10} if we neglected the influence of the lattice displacement. The amplitude of the oscillations in Fig. 10 is clearly too small to explain the experimental data, and they also have the wrong phase compared to Fig. 8.

These results demonstrate that nonuniform density effects play a decisive role in the observed transient optical response by eliminating the plasmon oscillations that dominate in the spatially homogeneous case. Another important finding is that the simplistic picture of the electro-optic effect based on (17) is inadequate for this transient regime, and that in fact the lattice dynamics and not the electric field *per se* determines the oscillatory optical response.

Mode beating

The experiment also indicates that at higher densities both LO and TO oscillations are present in the reflected signal, which results in a characteristic beating pattern.^{6,20} The observation of LO-TO beating is the most conclusive evidence for the inhomogeneous density effect. It is obvious from Fig. 1 that longitudinal oscillations with LO and TO frequencies cannot exist simultaneously at any single value of the density, so the only explanation for their coexistence is the presence of different densities in the region sampled by the probe beam. The mode beating effect is reproduced in our calculation if we in-

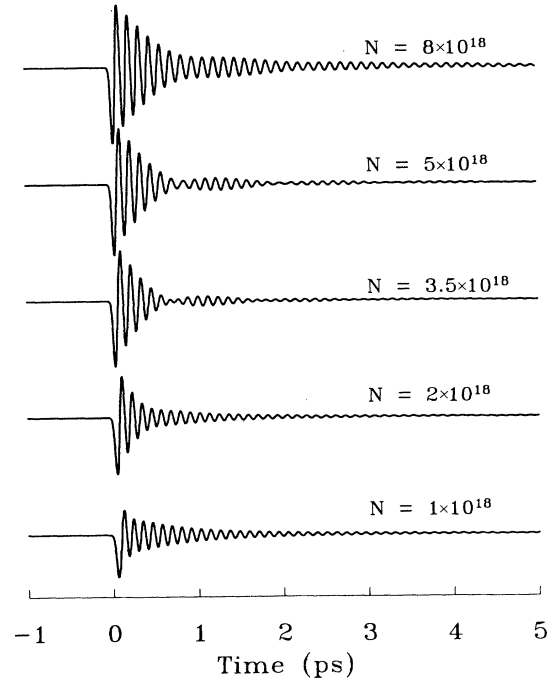


FIG. 11. Time derivative of the lattice displacement at high densities. The beating between LO and TO oscillations is clearly visible, and the damping becomes density dependent.

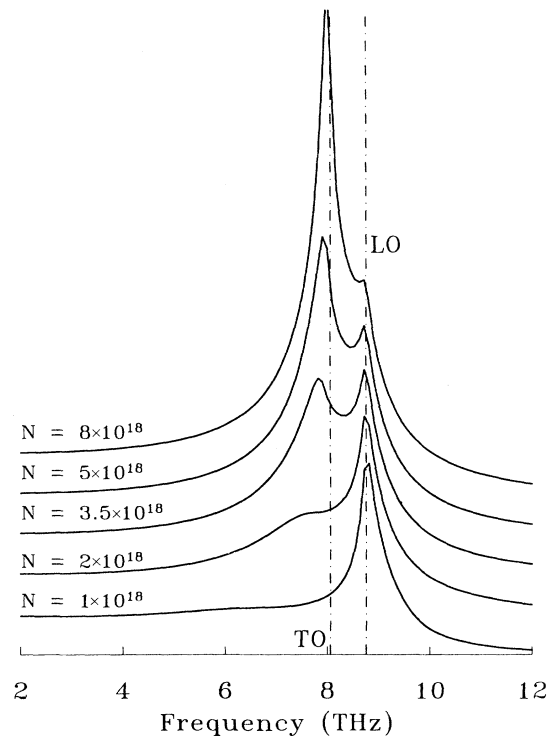


FIG. 12. Fourier transforms of the curves shown in Fig. 11. The TO mode is absent at low densities, but quickly becomes dominant at high densities. Note that the relative magnitude of the two peaks and their damping (spectral width) are density dependent, but their spectral position is not.

crease the densities by another order of magnitude.

In Fig. 11 we plot the time derivative of the lattice displacement for densities ranging from 1×10^{18} to $10 \times 10^{18} \text{ cm}^{-3}$. We have taken the derivative to eliminate the slow component of the response. Also, we concentrate on the lattice displacement and do not calculate the full response (18) because we expect the displacement to play a dominant role.

In this numerical example, the densities in the center of the laser spot are such that a well-defined longitudinal mode with TO frequency can exist (cf. Fig. 1). This mode competes with LO oscillations that are primarily produced at the wings of the density distribution. With growing density, the TO oscillations become comparable to the LO oscillations and eventually become dominant. This is clearly seen in Fig. 12, where the Fourier transform of the oscillatory patterns in Fig. 11 is plotted.

These results are qualitatively similar to recent experimental results²⁰ which confirm the above-described beating pattern. We would also like to point out that these are not “true” quantum beats where the same mode oscillates with two frequencies, but rather the result of interference between oscillations that occur in different places of the excited region.

Terahertz emission by coherent phonons

Rapid changes in current resulting from ultrafast optical excitation of dc-biased semiconductors lead to transient dipole electromagnetic radiation in the terahertz frequency range, as was experimentally and theoretically demonstrated in recent years.^{21–23} The radiation mostly results from fast initial rise of the polarization. However, as the above analysis demonstrates, there is also an oscillatory component in the polarization that in principle can result in a quasimonochromatic electromagnetic radiation at the phonon frequency.

Let us note that such radiation is very different from conventional polaritons¹⁵ which are transverse electromagnetic modes propagating *inside* the material. The polaritons do not create macroscopic dielectric polarization of the material and therefore do not emit dipole radiation. The electromagnetic transients we are concerned with here are observed in the far-field zone *outside* the material and are coherently produced by a collective motion of particles in the excited spot. Although technically this radiation is produced by *longitudinal* modes which would have been impossible in an idealized homogeneous situation, longitudinal oscillations of the polarization in a finite-size excited spot whose dimensions are smaller than the relevant wavelength constitute an experimental realization of a *Hertzian dipole oscillator* (see, e.g., Sec. 9.2 of Ref. 24) and can be treated accordingly.

In contrast to the electro-optic response discussed above, the radiated electric field E^{rad} is directly related to macroscopic polarization and hence to the time dependence of the electric field E in the material.²³

$$E^{\text{rad}}(r, t + r/c) = \frac{\sin\phi}{\epsilon_\infty c^2} \frac{V}{r} \frac{d^2 E}{dt^2}, \quad (19)$$

where ϕ is the angle of incidence, V the radiating volume,

and r the distance from the sample to the detector. Since we calculate the electric field dynamics in our numerical simulations, we can easily evaluate the radiated signal. According to Ref. 23, the effect of “nonvertical transitions”²² that are neglected in our model should be minimal for the relevant case of high dc fields and 2 eV excitation.

In Fig. 13 we plot the radiated field (19) for the case of high excitation density where the phonon oscillations (with the TO frequency, cf. Fig. 11) are most pronounced. We see that the radiation is still dominated by fast initial screening of the field, and the subsequent radiation at the TO frequency is about an order of magnitude weaker. The Fourier transform of this signal is shown in the inset. Note that, while the lattice dynamics at this density (the top curve in Figs. 11 and 12) is strongly dominated by TO oscillations, the electric field and the radiated transient contain LO, TO, and plasmon features.

Our results suggest that the role of phonon oscillations in the terahertz emission is expected to be minor. While in principle the magnitude of the oscillatory component in the radiated field (about 1 V/cm) is detectable by the dipole antennas used in terahertz experiments,²¹ it seems unlikely that such oscillations can be measured by this technique because the frequency response of the dipole antennas is limited to about 2 THz. However, the phonon feature in the frequency domain can potentially be detected by bolometric techniques²² which have wider bandwidth.

Very recently, Dekorsy *et al.*²⁵ have observed an electromagnetic terahertz transient from coherent phonons

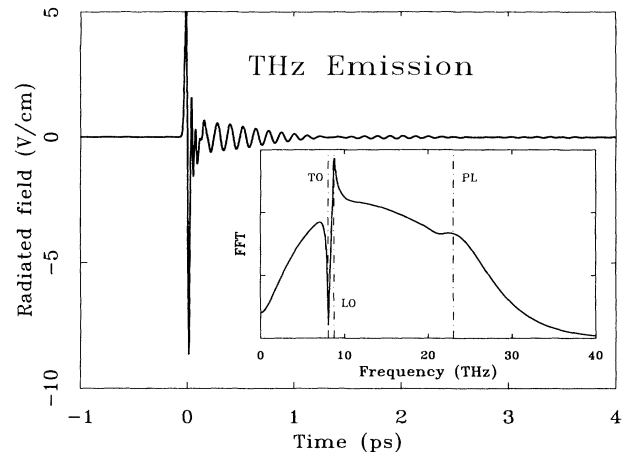


FIG. 13. Transient electromagnetic radiation for a high-density excitation ($N = 8 \times 10^{18} \text{ cm}^{-3}$; the top curve in Fig. 12) calculated according to Eq. (19). The radiating volume is assumed to be 10^{-9} cm^3 , $r = 1 \text{ cm}$, and $\phi = 45^\circ$. The initial transient is stronger than the subsequent oscillatory feature by about an order of magnitude even in this high-density example where the oscillations are most pronounced. In the frequency domain (inset), the LO and TO spectral features superimpose with a broad (up to 40 THz) response from the initial transient producing a peculiar dispersive shape of the overall signal. The plasmons are responsible for a small bump at 23 THz. In the time domain, fast plasmon oscillations are visible immediately after the initial transient.

in Te, where the phonon frequencies (about 2 THz) are within the spectral range of dipole antennas. This experiment indicates that the terahertz emission from coherent phonons is a quite general phenomenon and is not specific to GaAs or any other material.

IV. CONCLUSIONS

In this paper we have studied transient processes that follow ultrafast optical excitation of dc-biased polar semiconductors. By suddenly changing the dielectric properties of the material, optical excitation makes both the photoelectrons and the lattice oscillate around their new equilibrium positions. We have presented a microscopic theory that describes this oscillatory transient in terms of plasmon-phonon modes.

Our results can be summarized as follows. The physical quantities that perform the oscillations are the lattice displacement of the optical mode and the electronic polarization which are coupled to produce the well-known plasmon-phonon modes. The plasmons are much more effective in screening of the applied field because the phonons are relatively weakly coupled to the field. Therefore, in a generic case of uniform plasma density, the plasmon oscillations are found to be much stronger than the phonon ones.

However, the plasmon frequency is density dependent, and in a realistic experimental situation the plasmon oscillations are very strongly inhomogeneously broadened because regions of the excited spot with very different densities will contribute to the response. The effect of density inhomogeneity is to wash out plasmon oscillations while preserving density-independent LO-phonon features, which is consistent with the experimental findings. Although the plasmons do not show in the experimental curves, from the theoretical standpoint they are still very important because the plasmon period limits the rise time of electronic polarization and thus effectively controls the magnitude of the oscillatory response. A more careful experiment with controlled density distribution should be able to reveal both plasmons and phonons in the transient regime.

Although the inclusion of the inhomogeneous density effect gives the correct frequency of the oscillations, we were unable to reproduce the magnitude and phase of the oscillations in the differential reflectivity under the as-

sumption that the reflectivity is directly related to the instantaneous value of the electric field via the linear electro-optic effect¹⁰ [cf. Eq. (17)]. The amplitude of the field oscillations turns out to be too small compared to the applied field to explain the experimentally observed oscillatory response. However, the oscillating component in the lattice displacement is much stronger and is of the order of the observed response. After the influence of both the electric field and the displacement on the reflectivity is taken into account, the amplitude of the calculated oscillations becomes consistent with experiment.

At higher densities our theory predicts mode beating between LO oscillations from the fringes of the excited spot and TO oscillations from the high-density region in the center of the beam. Such LO-TO beating has been observed experimentally,^{6,20} which decisively confirms the presence of a wide range of densities in the excited spot.

The coherent oscillations in polarization should be a source for electromagnetic radiation at the phonon frequency.²⁵ Our calculation suggests that while this effect is measurable in principle, it is small compared to the broadband electromagnetic transient associated with quick initial screening of the applied field. The detection of such an oscillatory signal is also problematic because its frequency (10 THz) greatly exceeds the possibilities of conventional dipole antennas.

In conclusion, the coherent oscillations in GaAs can be quantitatively understood in terms of a plasmon-phonon picture. To describe the experimental data, the inclusion of the inhomogeneous density effect and a more accurate description of the electro-optic response are needed. However, nonlinear transport effects such as drift velocity saturation¹⁰ seem to play no role in the oscillatory response.

ACKNOWLEDGMENTS

The authors are grateful to T. Dekorsy and S. Obukhov for useful discussions. This work was supported by the U.S. Office of Naval Research through Grant No. N00091-JJ-1956 and by the NSF through Grant No. DMR 8957382. C.J.S. gratefully acknowledges support from the Alfred P. Sloan Foundation.

¹G. C. Cho, W. Kutt, and H. Kurz, *Phys. Rev. Lett.* **65**, 764 (1990).

²W. Kutt, G. C. Cho, T. Pfeifer, and H. Kurz, *Semicond. Sci. Technol.* **7**, B77 (1992).

³T. Pfeifer, W. Kutt, H. Kurz, and H. Scholz, *Phys. Rev. Lett.* **69**, 3248 (1992).

⁴T. K. Cheng, J. Vidal, H. J. Zeiger, G. Dresselhaus, M. S. Dresselhaus, and E. P. Ippen, *Appl. Phys. Lett.* **59**, 1923 (1991).

⁵W. Albrecht, Th. Kruse, and H. Kurz, *Phys. Rev. Lett.* **69**, 1451 (1992).

⁶W. A. Kutt, W. Albrecht, and H. Kurz, *IEEE J. Quantum Electron.* **QE-28**, 2434 (1992).

⁷H. J. Zeiger, J. Vidal, T. K. Cheng, E. P. Ippen, G. Dresselhaus, and M. S. Dresselhaus, *Phys. Rev.* **B45**, 768 (1992).

⁸A. V. Kuznetsov and C. J. Stanton, *Phys. Rev. Lett.* **73**, 3243 (1994).

⁹T. Pfeifer, T. Dekorsy, W. Kutt, and H. Kurz, *Appl. Phys. A* **55**, 482 (1992).

¹⁰T. Dekorsy, T. Pfeifer, W. Kutt, and H. Kurz, *Phys. Rev. B* **47**, 3842 (1993).

¹¹H. Heesel, S. Hunsche, H. Mikkelsen, T. Dekorsy, K. Leo, and H. Kurz, *Phys. Rev. B* **47**, 16000 (1993).

¹²T. Dekorsy, H. Heesel, T. Pfeifer, H. Mikkelsen, W. Kutt, K. Leo, and H. Kurz, *Opt. Soc. Am. Proc. Ultrafast Opt. Op-*

- toelectron. **14**, 129 (1993).
- ¹³R. Scholz and A. Stahl, *Phys. Status Solidi B* **168**, 123 (1991).
- ¹⁴A. Mooradian and A. L. McWhorter, *Phys. Rev. Lett.* **19**, 849 (1967).
- ¹⁵M. Born and K. Huang, *Dynamical Theory of Crystal Lattices* (Oxford University Press, Oxford, 1954).
- ¹⁶F. Vallee and F. Bogani, *Phys. Rev.* **B43**, 12 049 (1991).
- ¹⁷C. L. Collins and P. Y. Yu, *Solid State Commun.* **51**, 123 (1984).
- ¹⁸C. J. Stanton and D. W. Bailey, *Phys. Rev. B* **45**, 8369 (1992).
- ¹⁹C. H. Shih and A. Yariv, *J. Phys. C* **15**, 825 (1982).
- ²⁰T. Pfeifer, T. Dekorsy, W. Kutt, and H. Kurz, in *Phonon Scattering in Condensed Matter VII*, edited by M. Meissner and R. O. Pohl (Springer, Berlin, 1993), p. 110.
- ²¹X.-C. Zhang, B. B. Hu, J. T. Darrow, and D. H. Auston, *Appl. Phys. Lett.* **56**, 1101 (1990); B. B. Hu, A. S. Weling, D. H. Auston, A. V. Kuznetsov, and C. J. Stanton, *Phys. Rev. B* **49**, 2234 (1994).
- ²²S. L. Chuang, S. Schmitt-Rink, B. I. Greene, P. N. Saeta, and A. F. J. Levi, *Phys. Rev. Lett.* **68**, 102 (1992).
- ²³A. V. Kuznetsov and C. J. Stanton, *Phys. Rev. B* **48**, 10 828 (1993).
- ²⁴J. D. Jackson, *Classical Electrodynamics* (Wiley, New York, 1975).
- ²⁵T. Dekorsy, H. Auer, C. Waschke, H. J. Bakker, H. G. Roskos, H. Kurz, V. Vagner, and P. Grosse, *Phys. Rev. Lett.* **74**, 738 (1995).